

Variational Inference with Latent Space Quantization for Adversarial Resilience

Vinay Kyatham*
SigTuple Technologies
Bangalore, India

Mayank Mishra*, Tarun Kumar Yadav,
Deepak Mishra†, Prathosh AP†
Indian Institute of Technology Delhi
New Delhi, India

Abstract

Despite their tremendous success in modelling high-dimensional data manifolds, deep neural networks suffer from the threat of adversarial attacks - Existence of perceptually valid input-like samples obtained through careful perturbation that lead to degradation in the performance of the underlying model. Major concerns with existing defense mechanisms include non-generalizability across different attacks, models and large inference time. In this paper, we propose a generalized defense mechanism capitalizing on the expressive power of regularized latent space based generative models. We design an adversarial filter, devoid of access to classifier and adversaries, which makes it usable in tandem with any classifier. The basic idea is to learn a Lipschitz constrained mapping from the data manifold, incorporating adversarial perturbations, to a quantized latent space and re-map it to the true data manifold. Specifically, we simultaneously auto-encode the data manifold and its perturbations implicitly through the perturbations of the regularized and quantized generative latent space, realized using variational inference. We demonstrate the efficacy of the proposed formulation in providing resilience against multiple attack types (black and white box) and methods, while being almost real-time. Our experiments show that the proposed method surpasses the state-of-the-art techniques in several cases.

Introduction

Deep neural networks have shown tremendous success in various computer vision tasks. One of the primary factors contributing to their success is the availability of abundant data. This generally leads to an incomplete exploration of data space with the available training set, which in-turn results in loopholes in the data manifold (Gilmer et al. 2018; Schmidt et al. 2018). Adversarial attacks exploit these gaps in the data manifold, unexplored by the classifier which leads to the failure of otherwise successful networks. This unexplored subspace, called *adversarial subspace*, contains adversarial samples generated using perturbation of original training samples with carefully designed synthetic noise (Goodfellow, Shlens, and Szegedy 2014a; Szegedy et al. 2013; Moosavi-Dezfooli, Fawzi, and Frossard 2016; Carlini and Wagner 2017; Madry et al. 2017). This is an important

*Equal contribution

†Equal contribution

concern not only from a point of security but also from a generalization perspective (Tsipras et al. 2018). In the rest of the section, we will present an overview of the existing adversarial attacks, defense mechanisms along with the motivation for our work.

Adversarial attacks - General principles

An adversarial sample is obtained by perturbing the input sample with a small amount such that its perceptual quality is unaltered but the class label is changed under the classifier. Formally, let $\mathbf{x} \in \mathbb{R}^N$ denote a sample from the natural data manifold and $\mathbf{x}' = \mathbf{x} + \delta$, denote a perturbation on \mathbf{x} with $\delta \in \mathcal{S}$, $\mathcal{S} \subseteq \mathbb{R}^N$ being the space of all possible perturbations. Under a given distance metric \mathcal{D} and a classification scheme $h(\mathbf{x})$, the sample \mathbf{x}' is called an adversarial example for \mathbf{x} if $\mathcal{D}(\mathbf{x}, \mathbf{x}') \leq \epsilon$ and $h(\mathbf{x}) \neq h(\mathbf{x}')$. A large body of attacks consider a l_p -norm based \mathcal{D} , with l_2 and l_∞ norms being the significant ones, and solve an optimization problem on the loss function of $h(\mathbf{x})$ to obtain the desired δ . Attacks can be targeted so that the classifier is misguided to a specific class or non-targeted so that it outputs an arbitrary class different from the original class. Further categorization of adversarial attacks is based on the level of access the attacker has about the classification and defense scheme. Specifically they are defined as white and black box attacks.

Attack methods

There is a gamut of literature on creating adversarial attacks. Goodfellow, Shlens, and Szegedy propose Fast Gradient Sign Method (FGSM) that performs a one step gradient update along the direction of sign of gradient of loss at each pixel. Kurakin, Goodfellow, and Bengio introduced Basic Iterative method (BIM) which runs FGSM for a few iterations. Deepfool (Moosavi-Dezfooli, Fawzi, and Frossard 2016) is another iterative attack which computes adversarial perturbations through an orthogonal projection of the sample on the decision boundary. Carlini-Wagner (CW) attack (Carlini and Wagner 2017) is an optimization based attack that uses logits-based objective function instead of the commonly used cross-entropy loss. We choose these attacks since they cover a good breadth of the class of attacks.

Prior art on defense mechanisms

A large number of defense mechanisms to diminish the effect of adversarial attacks are available (Goodfellow et al.

2016; Samangouei, Kabkab, and Chellappa 2018; Ilyas et al. 2017; Song et al. 2017; Shen et al. 2017; Meng and Chen 2017; Madry et al. 2017; Papernot et al. 2016b). Broadly, these can be divided into the following categories -

1. **Adversarial retraining** - A natural way to make the classifier robust against the adversaries is to retrain the classifier using adversarial examples (Goodfellow et al. 2016; Szegedy et al. 2013). Several improvisations of adversarial retraining have been proposed (Madry et al. 2017; Sinha, Namkoong, and Duchi 2017; Tramèr et al. 2017). While adversarial retraining is a simple method for defense and is robust to first-order adversaries, it is shown to be ineffective towards DeepFool and CW attack (Tramèr et al. 2017) and also black-box attacks (Goodfellow, Shlens, and Szegedy 2014b; Sharma and Chen 2017; Ding et al. 2019)
2. **Modified training** - Here the idea is to tweak the training procedure and/or the training examples of the classifier so that the decision boundary learnt is robust to adversarial examples (Papernot et al. 2016b; Guo et al. 2017; Xiao et al. 2018; Dhillon et al. 2018; Xie et al. 2017). However, Athalye, Carlini, and Wagner demonstrate that most of these defenses are vulnerable because they capitalize on obfuscated gradients that can be mitigated.
3. **Adversarial filtering** - These defense mechanisms preprocess the adversarial examples to make them non-adversarial either by manifold projection or by using generative models. For example, MagNet (Meng and Chen 2017) trains a collection of detector networks that differentiate between normal and adversarial examples. It also includes a reformer network (one or a collection of auto-encoders) to push adversarial examples close to the data manifold. A recent strategy called Defense-GAN (Samangouei, Kabkab, and Chellappa 2018) trains a generative adversarial network (GAN) (Goodfellow et al. 2014) only on legitimate examples and uses it to denoise adversarial examples. At the time of inference, they find images from the range of generator that are near the input image but lie on the legitimate data manifold. This requires L iterations of back propagation for R random initializations to find the nearest legitimate image, typical value of L is 200 and R is 10. Other GAN based defences, for example, PixelDefend (Song et al. 2017) and APE-GAN (Shen et al. 2017), perform image-to-image translation to convert an adversarial image into a legitimate image.

Problem setting and our contributions

As mentioned, while the existing defense mechanisms have their own merits, each of them suffer from aforementioned disadvantages. Athalye, Carlini, and Wagner argue that most of these methods give a false sense of security since most of them capitalize on masking the gradients (obfuscated gradients) so that it is difficult to generate adversarial examples. However, they show that this can be circumvented using techniques such as approximation of derivatives by a differentiable approximation of the function, reparameterization and computation of expectations. In this paper, we propose a

defense mechanism based on quantized latent variable generative autoencoders to alleviate the aforementioned issues. Our contributions are enlisted below:

1. Propose a quantized latent variable generative model based defense mechanism devoid of access to classifier and adversaries.
2. Construction of a Lipschitz constrained latent encoder that preserves the distances under a metric space on the latent and the data manifolds.
3. Constraining the latent space to follow a known distribution so that stochastic exploration of the latent neighbourhood corresponding to the data neighbourhood is possible.
4. Use of dual decoders with a quantization on the latent space so that a large neighbourhood around a data sample is explored and easily remapped back to the data point.

Proposed Method

Motivation

In many previous works it is hypothesized that the adversarial examples fall off the data manifold (Lee, Han, and Lee 2017; Samangouei, Kabkab, and Chellappa 2018). This suggests that a defense model could potentially be built by replacing an adversarial example with the nearest correctly-classified sample from the data manifold. However, searching in high-dimensional data manifolds is expensive, not generalizable and moreover, it has been found that the adversarial examples might fall on the data manifold too (Gilmer et al. 2018). Thus, a better approach could be to project the data manifold onto an explorable compact generative latent space and remap the latent codes back to the legitimate data. If the latent space projector is made to be Lipschitz constrained and compact, then one can hope that the adversarial examples adhere to a latent code that is invertible to the legitimate data.

Lipschitz constrained latent transformation

Let $f(\mathbf{x}) : \mathbb{R}^N \rightarrow \mathbb{R}^M$ be a Lipschitz constrained function which maps a data point \mathbf{x} of dimension N to a latent vector \mathbf{z} of dimension M such that $M < N$. For such an f , if the adversarial perturbation δ on \mathbf{x} is bounded then the equivalent perturbation δ_z on \mathbf{z} is also bounded.

Since the goal is to learn mappings in high-dimensional spaces, we use Deep Neural Networks (DNNs) parameterized by θ , to approximate f_θ . There have been many methods proposed to make a DNN K -Lipschitz including gradient clipping (Arjovsky, Chintala, and Bottou 2017) and gradient norm penalty (Gulrajani et al. 2017). We employ gradient norm penalty on the encoder since it is observed to be more stable.

Latent exploration via variational inference

As mentioned earlier, the goal is to explore the latent neighbourhood induced by perturbing a given input sample. This effectively means that one has to sample from the true conditional distribution $p(\hat{\mathbf{z}}|\mathbf{x})$. However since there is no direct

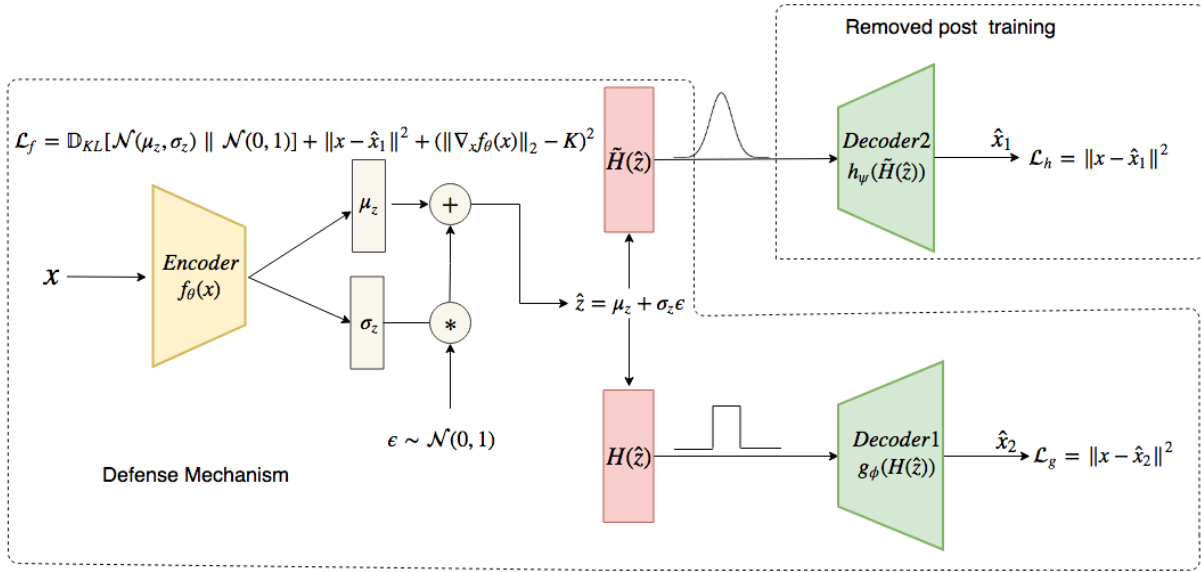


Figure 1: Proposed LQ-VAE - A Lipschitz constrained encoder (L_f) encodes the input image into a latent space quantized by the function H which is explored through a stochastic perturbation (ϵ). During inference, Decoder1 maps the quantized latent codes generated by the adversarial images back to the image space. Training is done **only on real data samples** by using an approximate differentiable version of Decoder1 (i.e. Decoder2).

access to $p(\hat{z}|\mathbf{x})$ we propose to use the principles of variational inference (Kingma and Welling 2013), where sampling from $p(\hat{z}|\mathbf{x})$ is facilitated by approximating it with a variational distribution $q_\theta(\hat{z}|\mathbf{x})$ on \hat{z} that is parameterized by the encoder network f_θ . Now minimizing the KL-divergence between $p(\hat{z}|\mathbf{x})$ and $q_\theta(\hat{z}|\mathbf{x})$ results in the maximization of the so-called evidence lower bound given as follows:

$$\mathcal{L} = \mathbb{E}_{q_\theta(\hat{z}|\mathbf{x})}[\log p_\phi(\mathbf{x}|\hat{z})] - \mathbb{D}_{KL}[q_\theta(\hat{z}|\mathbf{x})||p_\theta(\hat{z})] \quad (1)$$

where $p_\phi(\mathbf{x}|\hat{z})$ represents a probabilistic decoder network that maps the latent space back to the data space and $p_\theta(\hat{z})$ is an arbitrary prior on \hat{z} which is usually a Normal distribution. We propose to sample \hat{z} from $q_\theta(\hat{z}|\mathbf{x})$ using the encoder network f_θ through the reparameterization trick (Kingma and Welling 2013). Thus, given a true data example, a cloud of perturbations is created around its latent representation obtained through Lipschitz constrained encoder f_θ , via variational sampling. The probabilistic decoder $p_\phi(\mathbf{x}|\hat{z})$, parameterized using a neural network g_ϕ , is then tasked to map all the points within that cloud to a single input example through maximization of the likelihood term in (1), as shown in Figure 1. Mathematically, if the encoder embeds \mathbf{x} to a \hat{z} and $\mathbf{x} + \delta$ to a \hat{z}' , such that $\|\hat{z} - \hat{z}'\| \leq |\delta_z|$ then decoder learns $g_\phi(\hat{z}) = g_\phi(\hat{z}') = \mathbf{x}$. During inference, when the encoder is presented with an adversarial example, it will place it within the learned latent cloud so that the decoder converts it into a non-adversarial sample. This fact has been illustrated in Figure 2 where a 2D t-SNE plot of the latent encodings (from the Lipschitz constrained encoder) of the true and the CW l_2 attacked adversarial samples from the MNIST data is shown. It can be seen that embeddings of the adversaries are extremely close to those of the true samples.

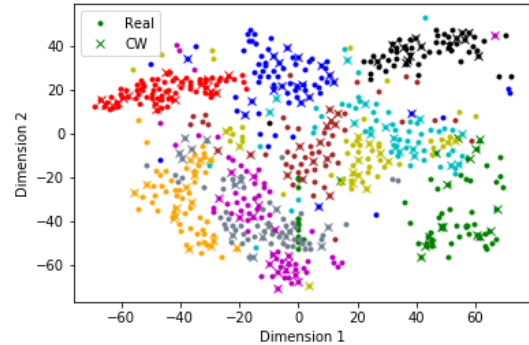


Figure 2: t-SNE plot of the latent encodings of mnist real images and CW adversarial images. It can be seen that the embeddings of real and adversarial data overlap.

Latent space quantization

A recent work by Gilmer et al. makes a very important observation - closeness from a correctly classified sample does not guarantee non-adversarial nature. In other words, since the latent space is real-valued it is impossible to explore it in its entirety. Thus, there is a high chance that a probabilistic decoder g_ϕ is unable to remove the adversarial noise even when the latent vector for an adversarial example falls within the seen latent cloud. We propose to address this issue by quantizing the latent space before it is input to the decoder. Specifically, we design a fixed discrete quantization function H applied on each dimension of the real-output of the

encoder as follows:

$$\mathbf{z}_i = H_i(\hat{\mathbf{z}}) = \begin{cases} +1 & \text{if } |\hat{\mathbf{z}}_i| \leq \eta \\ -1 & \text{otherwise} \end{cases} \quad (2)$$

where η is the quantization threshold. $H(\cdot)$ thus converts $\hat{\mathbf{z}}$ into binary coded vectors \mathbf{z} thereby ensuring that the decoder g_ϕ receives a single latent code for all the input samples that map within a small neighbourhood of $\hat{\mathbf{z}}$. In contrast to real $\hat{\mathbf{z}}$, where g_ϕ has to learn a non-injective mapping, quantization allows it to learn a mapping close to injective since the same code vector is produced for all $\hat{\mathbf{z}}$ in this neighbourhood, hence making the training easier. This procedure potentially increases the robustness of the model too since the goal of an adversarial resilience model is not to exactly reproduce the non-adversarial version of a given sample but to produce an approximate version that is non-adversarial. Thus, it is imperative to just look for the presence or absence of the salient features that preserve the identity of a given example, which is accomplished by the binary quantization with the threshold η being a hyperparameter whose value is chosen as, however not limited to, 0.67449 since it gives equal probability to a bit being +1 or -1. Thus, any deviation in the input sample falling outside the latent cloud leads to flipping of the bits in the quantized space.

Theorem 1 Let $\hat{\mathbf{z}}$ and $\hat{\mathbf{z}}_{adv}$ be the latent encoding of \mathbf{x} and \mathbf{x}_{adv} respectively. Let $\mathbf{z} = H(\hat{\mathbf{z}})$ and $\mathbf{z}_{adv} = H(\hat{\mathbf{z}}_{adv})$ be the corresponding quantizations. Then the probability of a particular bit being flipped is given by

$$p = \int_{\eta-|\delta_z|}^{\eta+|\delta_z|} p_{\hat{\mathbf{z}}}(\hat{\mathbf{z}}) d\hat{\mathbf{z}} \quad (3)$$

and the probability of $k = 6$ ($\approx 10\%$) bit flips for $M = 64$ dimensional latent space is $\binom{M}{k} p^k (1-p)^{M-k} = 1.177 \times 10^{-3}$ which is significantly low, when $\eta = 0.67449$ is chosen such that both bits are equally likely, $|\delta_z| = K|\delta| = 0.1 \times 0.3 = 0.03$ and $p_{\hat{\mathbf{z}}}(\hat{\mathbf{z}}) = \mathcal{N}(0, 1)$ (proof in supplementary material).

Figure 3 depicts the bit-flippings in the latent codes of the CW adversaries on the MNIST data - It can be seen that about 90 % of the total adversaries undergo less than 6% of bits being flipped resulting in high classification accuracy, confirming the effectiveness of the decoder in ignoring the bit-flippings. Further, the binary encoding layer ensures that gradient produced at that layer is either 0 or undefined, thereby making a gradient based attack on the defense mechanism impossible.

Adversarial resilience by LQ-VAE

As mentioned above, quantization prevents the flow of gradients through the encoder network f_θ that makes it non-trainable along with the decoder g_ϕ . We, therefore, create a copy of g_ϕ , say h_ψ , which uses soft quantization in place of H (called \tilde{H}) and enable the training of f_θ . A complete overview of the proposed method, called as Lipschitz-constrained quantized variational auto-encoder (LQ-VAE) is shown in Figure 1. Algorithm 1 gives the details of the LQ-VAE training procedure where the likelihood term in (1) is

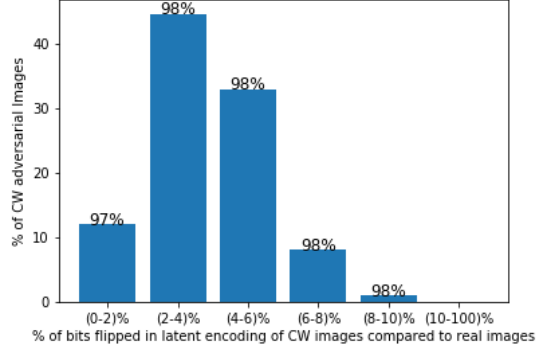


Figure 3: Effect of binary quantization on adversaries - It can be seen that more than 90 % of the adversaries have less than 6% of the bit flippings with high classification accuracy.

Algorithm 1 LQ-VAE algorithm

Input: Dataset \mathcal{D} , Batchsize B , Encoder f_θ , Decoder g_ϕ , Learning rate η , Quantization functions H, \tilde{H}
Output Parameters θ^*, ϕ^*

- 1: Make a copy h_ψ of decoder g_ϕ
 - 2: **repeat**
 - 3: Sample $\{\mathbf{x}^{(1)} \dots \mathbf{x}^{(B)}\}$ from dataset \mathcal{D}
 - 4: $\mu_{\mathbf{z}}, \sigma_{\mathbf{z}} \leftarrow f_\theta(\mathbf{x}^{(i)})$
 - 5: Sample $\hat{\mathbf{z}}^{(i)}$ from $\mathcal{N}(\mu_{\mathbf{z}}, \sigma_{\mathbf{z}}^{(i)2})$
 - 6: $\hat{\mathbf{x}}_1^{(i)} \leftarrow h_\psi(\tilde{H}(\hat{\mathbf{z}}^{(i)}))$
 - 7: $\hat{\mathbf{x}}_2^{(i)} \leftarrow g_\phi(H(\hat{\mathbf{z}}^{(i)}))$
 - 8: $\mathcal{L}_h \leftarrow \sum_{i=1}^B \left\| \mathbf{x}^{(i)} - \hat{\mathbf{x}}_1^{(i)} \right\|_2^2$
 - 9: $\mathcal{L}_g \leftarrow \sum_{i=1}^B \left\| \mathbf{x}^{(i)} - \hat{\mathbf{x}}_2^{(i)} \right\|_2^2$
 - 10: $\mathcal{L}_f \leftarrow \mathcal{L}_h + \sum_{i=1}^B \mathbb{D}_{KL} \left[\mathcal{N}(\mu_{\mathbf{z}}, \sigma_{\mathbf{z}}^{(i)2}) \parallel \mathcal{N}(0, 1) \right] + \sum_{i=1}^B \left[\left\| \nabla_x f_\theta(x^{(i)}) \right\|_2 - K \right]^2$
 - 11: $\theta \leftarrow \theta + \eta \nabla_\theta \mathcal{L}_f$
 - 12: $\phi \leftarrow \phi + \eta \nabla_\phi \mathcal{L}_g$
 - 13: $\psi \leftarrow \psi + \eta \nabla_\psi \mathcal{L}_h$
 - 14: **until** convergence of θ, ϕ
-

approximated using mean-squared error term between the input and the output. Note that the network h_ψ is only used for training, not for inference. The defense scheme only contains the pipeline of $f_\theta - H - g_\phi$.

Experiments and results

We consider MNIST (LeCun, Cortes, and Burges 2010), FMNIST¹, and CelebA (Liu et al. 2015) datasets and use three classifier architectures, named A, B, and C, for black box and white box experiments². For MNIST and FMNIST, the standard 10 class classification task is consid-

¹<https://github.com/zalandoresearch/fashion-mnist>

²Architectures of all the classifiers and LQ-VAE is included in supplementary material.

ered, whereas for CelebA, a binary classification task of gender classification is taken, with accuracy as the metric. Five attack types namely, FGSM with $\epsilon = 0.3$ (Goodfellow, Shlens, and Szegedy 2014a), l_2 CW (Carlini and Wagner 2017), Deepfool (Moosavi-Dezfooli, Fawzi, and Frossard 2016), iterative FGSM (Kurakin, Goodfellow, and Bengio 2016) and Madry (Madry et al. 2017), generated from clevrhans library (Papernot et al. 2016a), are considered for experimentation as they cover a good breadth of attack types. We compare our results with three defense strategies - Defense GAN (Samangouei, Kabkab, and Chellappa 2018), Madry (Madry et al. 2017) and Adversarial retraining (Goodfellow, Shlens, and Szegedy 2014a) based on the following facts (i) Defense GAN is close to our work in spirit. Their method also employs a generative model (GAN) and does not train on adversarial examples, (ii) Madry retraining is claimed to be a robust defense against all first-order gradient computation based attacks and (iii) adversarial retraining is one of the earliest benchmark defenses created. We use the Adam optimizer ($\beta_1 = 0.9, \beta_2 = 0.99$) with a learning rate of 10^{-3} to train LQ-VAE. We study different attack types, namely black box attacks, white box attack on classifier and end-to-end white box attack.

1. **Black box attacks** - The attacker neither has access to the original classifier nor the defense scheme, rather he has to generate adversarial examples on a substitute classifier (Papernot et al. 2017).
2. **White box attacks** - We subdivide white box attacks into two further categories:
 - (a) **White box attacks on classifier** - In this case, it is assumed that the attacker has access to the original classifier but not the defense scheme and the adversarial examples are generated by computing gradients over the original classifier.
 - (b) **White box attacks with BPDA** - The attacker has access to both the original classifier and the defense mechanism. In other words, the adversarial examples can be generated by computing gradients over the LQ-VAE - classifier combination. Athalye, Carlini, and Wagner argue that such methods can be attacked using Backward Pass Differentiable Approximation (BPDA). We attack the defense mechanism by approximating the discretization function $H(\hat{\mathbf{z}})$ with $\tilde{H}(\hat{\mathbf{z}})$ given as follows:

$$\tilde{H}_i(\hat{\mathbf{z}}) = \frac{\eta^2 - \hat{\mathbf{z}}_i^2}{c + |\eta^2 - \hat{\mathbf{z}}_i^2|} \quad (4)$$

where c is a non-negative hyperparameter. It can be seen that $H(\hat{\mathbf{z}}) = \tilde{H}(\hat{\mathbf{z}})$ when $c = 0$.

Results on white box attacks on classifier

For MNIST and FMNIST, we use 60,000 real images for training the defense mechanisms and 10,000 adversarial images on the standard test set for testing. For CelebA, we use 90% images for training and remaining for testing. Classification accuracy of all three classifier models, A, B, and C, in presence and absence of defense mechanisms are listed in

Table 1, 2, and 3 for MNIST, FMNIST, and CelebA, respectively. The attacks reduce classification accuracy of all the models drastically. Adversarial retraining is able to defend FGSM attack up to a certain extent but fails on the other attacks, since the retraining is performed using adversarial examples generated by FGSM attacks. Similarly Madry, which also uses first order gradients based adversarial images to retrain the classifiers, shows consistent performance against FGSM. However, for Deepfool and CW attack, its performance is lower than Defense-GAN and the proposed LQ-VAE. Both, Defense-GAN and LQ-VAE, do not require adversarial augmentation, however, we note that LQ-VAE consistently outperforms Defense-GAN.

Results on white box attacks with BPDA

Most of the defense mechanisms that rely on gradient obfuscation (Athalye, Carlini, and Wagner 2018) are broken completely by attacking using BPDA. However, Defense-GAN still has 55% accuracy on MNIST after the attack since it does not rely on gradient obfuscation. Our work is similar in spirit to Defense-GAN in this sense that it also does not rely on gradient obfuscation. We generate adversarial examples for the LQ-VAE - classifier combination via BPDA, however, passing these examples to the Lipschitz constrained encoder still results in these adversarial examples getting the same discrete latent codes (refer Figure 3 and Theorem 1) as their non-adversarial counterparts and thus their non-adversarial counterparts are successfully reconstructed by the decoder resulting in their correct classification (refer Table 7). We compare our results with Defense-GAN since Athalye, Carlini, and Wagner show that it can also be attacked using BPDA.

Results on black box attacks

For black box experiments, we consider one attack each on a dataset as a representative set. Specifically, FGSM for MNIST, Deepfool for FMNIST and CW for CelebA are considered with six-pairs of classifiers used for attacking and substitute. A similar trend is observed with the black box attacks as well, as seen in Tables 4, 5 and 6. Madry retraining performs the best on the FGSM attack because it is trained on a superset of first-order methods of which FGSM is a subset. However, the performance of LQ-VAE is consistent irrespective of the classifier pairs across all cases and is closely comparable (or better) to the best case. On Deepfool and CW, LQ-VAE outperforms the others in most of the cases. We hypothesize that this behaviour of LQ-VAE comes from the Lipschitz constraining, by which it becomes a strong defense when the attack alters fewer pixels of the input image yet changing the class, as in the case of CW and Deepfool, unlike in FGSM. In summary, the proposed method is invariant to white or black box attack types.

Discussions and Conclusions

LQ-VAE and Defense-GAN fall into the same category of defense mechanisms in the sense that they both capitalize on the expressive capacity of generative models. Further,

Attack	Model	No Attack	No Defense	LQ-VAE	Defense-GAN	Madry	Adv Tr
FGSM	A	92.76	11.50	77.00	69.75	78.87	53.72
	B	91.17	10.14	69.41	56.72	76.94	59.79
	C	89.06	11.60	67.07	56.34	64.16	66.43
Deepfool	A	92.76	5.29	79.30	77.48	57.17	6.52
	B	91.17	6.54	79.41	74.97	52.58	14.74
	C	89.06	7.65	79.89	74.82	39.93	24.71
CW	A	92.76	5.41	80.64	78.75	62.55	5.35
	B	91.17	6.61	81.58	78.18	56.48	6.35
	C	89.06	7.89	82.31	78.58	43.72	8.00
Average		91.00	8.07	77.40	71.73	59.15	27.29

Table 1: Classification accuracy of the FMNIST classifiers on white box attacks with various defense strategies

Attack	Model	No Attack	No Defense	LQ-VAE	Defense-GAN	Madry	Adv Tr
FGSM	A	99.40	20.16	89.17	90.43	96.85	67.95
	B	99.41	13.17	86.70	88.52	96.20	49.49
	C	98.37	5.66	83.02	86.7	84.71	80.75
Deepfool	A	99.40	7.38	97.60	95.41	67.82	3.10
	B	99.41	5.88	97.74	93.03	66.35	5.75
	C	98.37	48.24	97.42	92.32	62.38	10.97
CW	A	99.40	8.85	97.66	94.37	69.15	1.20
	B	99.41	5.07	97.20	90.56	71.35	1.45
	C	98.37	8.44	97.36	92.5	58.65	2.15
Average		99.06	13.65	93.76	91.54	74.83	24.76

Table 2: Classification accuracy of the MNIST classifiers on white box attacks with various defense strategies.

Attack	Model	No Attack	No Defense	LQ-VAE	Defense-GAN	Madry	Adv Tr
FGSM	A	96.34	3.65	81.04	74.13	62.35	4.53
	B	96.60	3.40	64.74	67.06	71.42	72.88
	C	95.02	28.62	61.48	53.76	61.35	42.55
Deepfool	A	96.34	3.56	85.89	83.87	52.86	6.26
	B	96.60	2.43	83.81	83.65	49.39	14.17
	C	95.02	10.92	62.79	78.56	42.37	38.45
CW	A	96.34	6.98	85.90	84.64	58.62	11.88
	B	96.60	6.88	86.29	86.01	60.33	12.91
	C	95.02	10.92	79.20	78.56	45.02	38.45
Iter FGSM	A	96.34	3.12	85.44	81.00	82.34	3.50
	B	96.60	3.55	72.29	72.05	72.19	9.16
	C	95.02	11.92	52.12	42.13	90.87	19.47
Madry	A	96.34	2.84	85.11	81.43	76.35	3.52
	B	96.60	3.12	70.01	74.01	70.32	8.52
	C	95.02	8.57	54.00	45.11	84.09	18.59
Average		95.99	7.37	74.01	72.40	65.32	20.32

Table 3: Classification accuracy of the CelebA classifiers on white box attacks with various defense strategies.

both of the models generalize better on the adaptive or unseen attacks (Athalye, Carlini, and Wagner 2018) since both of them neither need access to the classifier nor train on a certain type of adversaries. However, LQ-VAE offers several advantages over Defense-GAN such as - (i) LQ-VAE does not involve a run-time search on the latent space unlike Defense-GAN which makes it orders of magnitude faster and independent of latent search parameters. Rather in LQ-

VAE, the search in the latent space is implicitly done by effective encoding, quantization and decoding of the latent space. (ii) training a VAE is known to be easier and faster, yielding a better data likelihood than a GAN which is known to be difficult to be trained, especially on color datasets such as CelebA, (iii) LQ-VAE has a latent encoding followed by the re-mapping of the latent space to the data space which makes it invariant to attack types while Defense-GAN is

Classifier Substitute	No Attack	No Defense	LQ-VAE	Defense-GAN	Madry	Adv Tr
A/B	99.40	33.32	88.09	89.14	97.17	95.78
A/C	99.40	45.35	90.60	90.08	98.27	96.82
B/A	99.41	42.22	90.63	91.40	97.38	94.64
B/C	99.41	38.73	89.92	89.89	98.03	95.30
C/A	98.37	28.93	91.98	90.90	90.59	32.12
C/B	98.37	18.01	89.38	88.73	89.14	21.79
Average	99.06	34.43	90.10	90.02	95.10	72.74

Table 4: Classification accuracy of the MNIST classifier on FGSM black box attack images generated using substitute model.

Classifier/ Substitute	No Attack	No Defense	LQ-VAE	Defense-GAN	Madry	Adv Tr
A/B	92.76	29.14	77.74	74.41	60.11	48.27
A/C	92.76	35.44	77.11	74.11	62.58	57.53
B/A	91.17	67.82	81.33	77.97	80.71	76.61
B/C	91.17	45.55	78.83	74.5	69.19	64.05
C/A	89.06	79.11	82.12	78.82	80.99	81.84
C/B	89.06	47.26	80.76	76.6	67.46	59.64
Average	91.00	50.72	79.65	76.07	70.17	64.66

Table 5: Classification accuracy of the FMNIST classifier on Deepfool black box attack images generated using substitute model.

Classifier/ Substitute	No Attack	No Defense	LQ-VAE	Defense-GAN	Madry	Adv Tr
A/B	96.34	39.53	86.01	84.70	85.41	94.13
A/C	96.34	37.59	80.10	78.11	64.72	54.22
B/A	96.60	49.21	85.67	86.19	82.55	68.11
B/C	96.60	52.52	79.98	79.91	76.31	62.53
C/A	95.02	82.87	85.90	86.29	89.79	86.75
C/B	95.02	83.26	85.20	86.17	89.91	88.40
Average	95.99	57.50	83.81	83.56	81.45	75.69

Table 6: classification accuracy of the CelebA classifier on CW black box attack images generated using substitute model

Dataset	LQ-VAE	Defense-GAN
MNIST	83.70	55.17
FMNIST	57.41	39.41

Table 7: Classification accuracy of end-to-end whitebox FGSM attack on LQ-VAE - classifier combination using BPDA.

shown to degrade in the case of black box attacks, (iv) as argued in (Athalye, Carlini, and Wagner 2018), Defense-GAN can be attacked too by a method called the Backward Pass Differentiable Approximation (BPDA), in which case its defense on MNIST is reported at 55% (Athalye, Carlini, and Wagner 2018). When the same technique is used to attack LQ-VAE, we get much better accuracy of 83% on the same task which can be ascribed to the use of latent space constraining and quantization. In summary, we proposed a technique called LQ-VAE as a filter for the adversarial examples using a constrained projection on to a quantized latent space

followed by data reconstruction. It serves like a ‘black-box defense’ in the sense that it can be used to defend any attack and with any classifier. In principle, LQ-VAE can be re-trained using adversaries too, in which case the performance is observed to improve. For instance, it is observed that if one retrains LQ-VAE using Madry adversaries, its performance is enhanced by 5-10% on FGSM attacks. Future directions include exploration of the latent prior p_θ beyond a standard Normal distribution, studying the effect of different types of quantization other than a simple binary quantization and using LQ-VAE as an adversarial detector. We provide the code³ for further research.

References

[Arjovsky, Chintala, and Bottou 2017] Arjovsky, M.; Chintala, S.; and Bottou, L. 2017. Wasserstein gan. *arXiv preprint arXiv:1701.07875*.

³The code used in this paper can be accessed at <https://github.com/mayank31398/lqvae>

- [Athalye, Carlini, and Wagner 2018] Athalye, A.; Carlini, N.; and Wagner, D. 2018. Obfuscated gradients give a false sense of security: Circumventing defenses to adversarial examples. *arXiv preprint arXiv:1802.00420*.
- [Carlini and Wagner 2017] Carlini, N., and Wagner, D. 2017. Towards evaluating the robustness of neural networks. In *2017 IEEE Symposium on Security and Privacy (SP)*, 39–57. IEEE.
- [Dhillon et al. 2018] Dhillon, G. S.; Azizzadenesheli, K.; Lipton, Z. C.; Bernstein, J.; Kossaifi, J.; Khanna, A.; and Anandkumar, A. 2018. Stochastic activation pruning for robust adversarial defense. *arXiv preprint arXiv:1803.01442*.
- [Ding et al. 2019] Ding, G. W.; Lui, K. Y. C.; Jin, X.; Wang, L.; and Huang, R. 2019. On the sensitivity of adversarial robustness to input data distributions. *arXiv preprint arXiv:1902.08336*.
- [Gilmer et al. 2018] Gilmer, J.; Metz, L.; Faghri, F.; Schoenholz, S. S.; Raghu, M.; Wattenberg, M.; and Goodfellow, I. 2018. Adversarial spheres. *arXiv preprint arXiv:1801.02774*.
- [Goodfellow et al. 2014] Goodfellow, I.; Pouget-Abadie, J.; Mirza, M.; Xu, B.; Warde-Farley, D.; Ozair, S.; Courville, A.; and Bengio, Y. 2014. Generative adversarial nets. In *Advances in neural information processing systems*, 2672–2680.
- [Goodfellow et al. 2016] Goodfellow, I.; Bengio, Y.; Courville, A.; and Bengio, Y. 2016. *Deep learning*, volume 1. MIT Press.
- [Goodfellow, Shlens, and Szegedy 2014a] Goodfellow, I. J.; Shlens, J.; and Szegedy, C. 2014a. Explaining and harnessing adversarial examples. *arXiv preprint arXiv:1412.6572*.
- [Goodfellow, Shlens, and Szegedy 2014b] Goodfellow, I. J.; Shlens, J.; and Szegedy, C. 2014b. Explaining and Harnessing Adversarial Examples. *arXiv e-prints arXiv:1412.6572*.
- [Gulrajani et al. 2017] Gulrajani, I.; Ahmed, F.; Arjovsky, M.; Dumoulin, V.; and Courville, A. C. 2017. Improved training of wasserstein gans. In *Advances in Neural Information Processing Systems*, 5767–5777.
- [Guo et al. 2017] Guo, C.; Rana, M.; Cisse, M.; and van der Maaten, L. 2017. Countering adversarial images using input transformations. *arXiv preprint arXiv:1711.00117*.
- [Ilyas et al. 2017] Ilyas, A.; Jalal, A.; Asteri, E.; Daskalakis, C.; and Dimakis, A. G. 2017. The robust manifold defense: Adversarial training using generative models. *arXiv preprint arXiv:1712.09196*.
- [Kingma and Welling 2013] Kingma, D. P., and Welling, M. 2013. Auto-encoding variational bayes. *arXiv preprint arXiv:1312.6114*.
- [Kurakin, Goodfellow, and Bengio 2016] Kurakin, A.; Goodfellow, I.; and Bengio, S. 2016. Adversarial examples in the physical world. *arXiv preprint arXiv:1607.02533*.
- [LeCun, Cortes, and Burges 2010] LeCun, Y.; Cortes, C.; and Burges, C. 2010. Mnist handwritten digit database. *AT&T Labs [Online]*. Available: <http://yann.lecun.com/exdb/mnist> 2.
- [Lee, Han, and Lee 2017] Lee, H.; Han, S.; and Lee, J. 2017. Generative adversarial trainer: Defense to adversarial perturbations with gan. *arXiv preprint arXiv:1705.03387*.
- [Liu et al. 2015] Liu, Z.; Luo, P.; Wang, X.; and Tang, X. 2015. Deep learning face attributes in the wild. In *Proceedings of the IEEE International Conference on Computer Vision*, 3730–3738.
- [Madry et al. 2017] Madry, A.; Makelov, A.; Schmidt, L.; Tsipras, D.; and Vladu, A. 2017. Towards deep learning models resistant to adversarial attacks. *arXiv preprint arXiv:1706.06083*.
- [Meng and Chen 2017] Meng, D., and Chen, H. 2017. Magnet: a two-pronged defense against adversarial examples. In *Proceedings of the 2017 ACM SIGSAC Conference on Computer and Communications Security*, 135–147. ACM.
- [Moosavi-Dezfooli, Fawzi, and Frossard 2016] Moosavi-Dezfooli, S.-M.; Fawzi, A.; and Frossard, P. 2016. Deepfool: a simple and accurate method to fool deep neural networks. In *Proceedings of the IEEE Conference on Computer Vision and Pattern Recognition*, 2574–2582.
- [Papernot et al. 2016a] Papernot, N.; Goodfellow, I.; Sheth, R.; Feinman, R.; and McDaniel, P. 2016a. cleverhans v1.0.0: an adversarial machine learning library. *arXiv preprint arXiv:1610.00768*.
- [Papernot et al. 2016b] Papernot, N.; McDaniel, P.; Wu, X.; Jha, S.; and Swami, A. 2016b. Distillation as a defense to adversarial perturbations against deep neural networks. In *2016 IEEE Symposium on Security and Privacy (SP)*, 582–597. IEEE.
- [Papernot et al. 2017] Papernot, N.; McDaniel, P.; Goodfellow, I.; Jha, S.; Celik, Z. B.; and Swami, A. 2017. Practical black-box attacks against machine learning. In *Proceedings of the 2017 ACM on Asia Conference on Computer and Communications Security*, 506–519. ACM.
- [Samangouei, Kabkab, and Chellappa 2018] Samangouei, P.; Kabkab, M.; and Chellappa, R. 2018. Defense-gan: Protecting classifiers against adversarial attacks using generative models.
- [Schmidt et al. 2018] Schmidt, L.; Santurkar, S.; Tsipras, D.; Talwar, K.; and Madry, A. 2018. Adversarially robust generalization requires more data. In *Advances in Neural Information Processing Systems*, 5019–5031.
- [Sharma and Chen 2017] Sharma, Y., and Chen, P.-Y. 2017. Attacking the madry defense model with l_1 -based adversarial examples. *arXiv preprint arXiv:1710.10733*.
- [Shen et al. 2017] Shen, S.; Jin, G.; Gao, K.; and Zhang, Y. 2017. Ape-gan: Adversarial perturbation elimination with gan. *arXiv preprint arXiv:1707.05474*.
- [Sinha, Namkoong, and Duchi 2017] Sinha, A.; Namkoong, H.; and Duchi, J. 2017. Certifying some distributional robustness with principled adversarial training. *arXiv preprint arXiv:1710.10571*.
- [Song et al. 2017] Song, Y.; Kim, T.; Nowozin, S.; Ermon, S.; and Kushman, N. 2017. Pixeldefend: Leveraging generative models to understand and defend against adversarial examples. *arXiv preprint arXiv:1710.10766*.

[Szegedy et al. 2013] Szegedy, C.; Zaremba, W.; Sutskever, I.; Bruna, J.; Erhan, D.; Goodfellow, I.; and Fergus, R. 2013. Intriguing properties of neural networks. *arXiv preprint arXiv:1312.6199*.

[Tramèr et al. 2017] Tramèr, F.; Kurakin, A.; Papernot, N.; Goodfellow, I.; Boneh, D.; and McDaniel, P. 2017. Ensemble adversarial training: Attacks and defenses. *arXiv preprint arXiv:1705.07204*.

[Tsipras et al. 2018] Tsipras, D.; Santurkar, S.; Engstrom, L.; Turner, A.; and Madry, A. 2018. Robustness may be at odds with accuracy. *stat* 1050:11.

[Xiao et al. 2018] Xiao, K. Y.; Tjeng, V.; Shafiqullah, N. M.; and Madry, A. 2018. Training for faster adversarial robustness verification via inducing relu stability. *arXiv preprint arXiv:1809.03008*.

[Xie et al. 2017] Xie, C.; Wang, J.; Zhang, Z.; Ren, Z.; and Yuille, A. 2017. Mitigating adversarial effects through randomization. *arXiv preprint arXiv:1711.01991*.

Appendix

Proof for Theorem 1

Let $\hat{\mathbf{z}}$ and $\hat{\mathbf{z}}_{adv}$ be the latent encoding of \mathbf{x} and \mathbf{x}_{adv} respectively. Let $\mathbf{z} = H(\hat{\mathbf{z}})$ and $\mathbf{z}_{adv} = H(\hat{\mathbf{z}}_{adv})$ be the corresponding quantizations with η being the quantization threshold. Then the probability of a particular bit being flipped is given by:

$$p = \underbrace{P(\mathbf{z} = -1, \mathbf{z}_{adv} = 1)}_A + \underbrace{P(\mathbf{z} = 1, \mathbf{z}_{adv} = -1)}_B \quad (5)$$

$$\begin{aligned} A &= P(\hat{\mathbf{z}} < -\eta, -\eta < \hat{\mathbf{z}}_{adv} < \eta) \\ &\quad + P(\hat{\mathbf{z}} > \eta, -\eta < \hat{\mathbf{z}}_{adv} < \eta) \\ &= P(\hat{\mathbf{z}} < -\eta, -\eta - \delta_z < \hat{\mathbf{z}} < \eta - \delta_z) \\ &\quad + P(\hat{\mathbf{z}} > \eta, -\eta - \delta_z < \hat{\mathbf{z}} < \eta - \delta_z) \end{aligned} \quad (6)$$

$$\begin{aligned} &= \begin{cases} \int_{-\eta-\delta_z}^{-\eta} p_{\hat{\mathbf{z}}}(\hat{\mathbf{z}}) d\hat{\mathbf{z}} & \text{if } \delta_z \geq 0 \\ \int_{\eta}^{\eta-\delta_z} p_{\hat{\mathbf{z}}}(\hat{\mathbf{z}}) d\hat{\mathbf{z}} & \text{otherwise} \end{cases} \\ &= \int_{\eta}^{\eta+|\delta_z|} p_{\hat{\mathbf{z}}}(\hat{\mathbf{z}}) d\hat{\mathbf{z}} \end{aligned}$$

which is obtained by using $p_{\hat{\mathbf{z}}}(\hat{\mathbf{z}}) = \mathcal{N}(0, 1)$ which is an even function. Similarly,

$$B = \int_{\eta-|\delta_z|}^{\eta} p_{\hat{\mathbf{z}}}(\hat{\mathbf{z}}) d\hat{\mathbf{z}} \quad (7)$$

Adding A and B we have,

$$p = \int_{\eta-|\delta_z|}^{\eta+|\delta_z|} p_{\hat{\mathbf{z}}}(\hat{\mathbf{z}}) d\hat{\mathbf{z}} \quad (8)$$

To give equal probability to \mathbf{z} taking the values -1 or 1 we have the following constraint:

$$P(\mathbf{z} = 1) = \int_{-\eta}^{\eta} p_{\hat{\mathbf{z}}}(\hat{\mathbf{z}}) d\hat{\mathbf{z}} = 0.5 \quad (9)$$

Solving this for $p_{\hat{\mathbf{z}}}(\hat{\mathbf{z}}) = \mathcal{N}(0, 1)$, we have $\eta = 0.67449$. Using this value of η and $|\delta_z| = K|\delta|$ we get $|\delta_z| = 0.03$ where $K = 0.1$ is the Lipschitz constant and $|\delta| = 0.3$ is the perturbation in the input image. Thus, the probability of a bit being flipped is found to be $p = 0.01906$ which is a significantly low number. For a M dimensional latent space, the probability of k bit flips is $\binom{M}{k} p^k (1-p)^{M-k}$ which is found to be 1.177×10^{-3} for $k = 6$ ($\approx 10\%$) bit flips for a $M = 64$ dimensional latent space.

Architectures of the classifier and substitute networks

The following table shows the neural network architectures used throughout the paper for classifier and substitute models. Terminology used:

- Conv($m, f \times f, s$) denotes a convolutional layer with m filters of size $f \times f$ and stride s
- ReLu is the Rectified Linear Unit Activation
- LeakyReLu(α) is the Leaky Rectified Linear Unit Activation with parameter α
- Dropout(p) is a dropout layer with probability p
- FC(m) denotes a fully connected layer with m neuron units
- ConvT($m, f \times f, s$) denotes a deconvolutional layer with m filters of size $f \times f$ and stride s

A	B	C
Conv(64, 5×5 , 1)	Dropout(0.2)	FC(200)
ReLu	Conv(64, 8×8 , 2)	ReLu
Conv(64, 5×5 , 2)	ReLu	Dropout(0.5)
ReLu	Conv(128, 6×6 , 2)	FC(200)
Dropout(0.25)	ReLu	ReLu
FC(128)	Conv(128, 5×5 , 1)	FC(*)
ReLu	ReLu	Softmax
Dropout(0.5)	Dropout(0.5)	
FC(*)	FC(*)	
Softmax	Softmax	

Final Fully connected layer has 10 units for MNIST and FMNIST and 2 units for CelebA dataset.

LQ-VAE architecture

Encoder	Decoder1 \ Decoder2
Conv(64, 3×3 , 1)	FC(1024)
LeakyReLu(0.2)	LeakyReLu(0.2)
Conv(64, 3×3 , 2)	FC(6272)
LeakyReLu(0.2)	LeakyReLu(0.2)
Conv(128, 3×3 , 2)	ConvT(128, 3×3 , 1)
LeakyReLu(0.2)	LeakyReLu(0.2)
Conv(128, 3×3 , 1)	ConvT(128, 3×3 , 2)
LeakyReLu(0.2)	LeakyReLu(0.2)
FC(1024)	ConvT(64, 3×3 , 2)
LeakyReLu(0.2)	LeakyReLu(0.2)
FC(64), FC(64)	ConvT(1, 3×3 , 1)

Table 8: The encoder and decoder of LQ-VAE used in the experiments on MNIST and Fashion-MNIST

Encoder	Decoder1 \ Decoder2
Conv(64, 3 × 3, 1)	FC(1024)
LeakyReLu(0.2)	LeakyReLu(0.2)
Conv(64, 3 × 3, 2)	FC(4096)
LeakyReLu(0.2)	LeakyReLu(0.2)
Conv(128, 3 × 3, 2)	ConvT(128, 3 × 3, 2)
LeakyReLu(0.2)	LeakyReLu(0.2)
Conv(128, 3 × 3, 2)	ConvT(128, 3 × 3, 2)
LeakyReLu(0.2)	LeakyReLu(0.2)
Conv(256, 3 × 3, 2)	ConvT(64, 3 × 3, 2)
LeakyReLu(0.2)	LeakyReLu(0.2)
FC(1024)	ConvT(64, 3 × 3, 2)
LeakyReLu(0.2)	LeakyReLu(0.2)
FC(64), FC(64)	ConvT(3, 3 × 3, 1)

Table 9: The encoder and decoder of LQ-VAE used in the experiments on CelebA